

Applicability of condensation particle counters to measure atmospheric clusters

M. Sipilä^{1,2}, K. Lehtipalo¹, M. Kulmala¹, T. Petäjä^{1,*}, H. Junninen¹, P. P. Aalto¹,
H. E. Manninen¹, E. Vartiainen¹, I. Riipinen¹, E.-M. Kyrö¹, J. Curtius^{3,**},
A. Kürten^{4,***}, S. Borrmann^{3,4}, and C. D. O'Dowd⁵

¹Department of Physical Sciences, University of Helsinki, Finland

²Helsinki Institute of Physics, Helsinki, Finland

³Institute for Atmospheric Physics, J. Gutenberg-University Mainz, Mainz, Germany

⁴Max Planck Institute for Chemistry, Particle Chemistry Department, Mainz, Germany

⁵School of Physics & Centre for Climate and Air Pollution Studies, Environmental Change Institute, National University of Ireland, Galway, Ireland

* now at: Earth and Sun Systems Laboratory, Atmospheric Chemistry Division, National Center for Atmospheric Research, Boulder, USA

** now at: Institute for Atmosphere and Environment, J. W. Goethe-University Frankfurt, Frankfurt am Main, Germany

*** now at: Division of Engineering and Applied Science, California Institute of Technology, Pasadena, CA, USA

Received: 19 November 2007 – Accepted: 28 January 2008 – Published: 3 March 2008

Correspondence to: M. Sipilä (mikko.sipila@helsinki.fi)

Atmospheric cluster measurements

M. Sipilä et al.

Title Page

Abstract

Introduction

Conclusions

References

Tables

Figures

◀

▶

◀

▶

Back

Close

Full Screen / Esc

Printer-friendly Version

Interactive Discussion

EGU

Abstract

The ambient and laboratory molecular and ion clusters were investigated. Here we present data on the ambient concentrations of both charged and uncharged molecular clusters as well as the performance of a pulse height condensation particle counter (PH-CPC) and an expansion condensation particle counter (E-CPC). The ambient molecular cluster concentrations were measured using both instruments, and they were deployed in conjunction with ion spectrometers and other aerosol instruments in Hyytiälä, Finland at the SMEAR II station during 1 March to 30 June 2007. The observed cluster concentrations varied and were from ca. 1000 to 100 000 cm⁻³. Both instruments showed similar concentrations. The average size of detected clusters was approximately 1.8 nm. As the atmospheric measurements at sub 2-nm particles and molecular clusters are a challenging task, and we were most likely unable to detect the smallest clusters, the reported concentrations are our best estimates for minimum cluster concentrations in boreal forest environment.

1 Introduction

An important phenomenon associated with the atmospheric aerosol system is the formation of new atmospheric aerosol particles (Kulmala, 2003). Atmospheric aerosol formation involves a complicated set of processes that include the production of nanometer-size clusters from gaseous vapours, the growth of these clusters to detectable sizes, and their simultaneous removal by coagulation with the pre-existing aerosol particle population (e.g. Kerminen et al., 2001; Kulmala, 2003). Once formed, aerosol particles need to grow further to sizes larger than 50–100 nm in diameter until they are able to influence climate, even though smaller particles may have influences on human health and atmospheric chemistry. While aerosol formation has been observed to take place almost everywhere in the atmosphere (Kulmala et al., 2004a), serious gaps in our knowledge regarding this phenomenon still exist. These gaps include

Atmospheric cluster measurements

M. Sipilä et al.

Title Page

Abstract

Introduction

Conclusions

References

Tables

Figures

◀

▶

◀

▶

Back

Close

Full Screen / Esc

Printer-friendly Version

Interactive Discussion

existence and dynamics of atmospheric molecular clusters, vapours participating on atmospheric cluster formation, the effect of those clusters on atmospheric nucleation, the effect of ions on particle formation and also the various impacts of new particle formation on atmospheric chemistry, climate, human health and environment.

Although some investigations have been promising (see e.g. Kulmala et al., 2005a) critical clusters formed during atmospheric nucleation events have not been measured quantitatively until recently (Kulmala et al., 2007a) due to instrumental limitations. Only some measurements of clusters during nucleation events have been reported. Weber et al. (1995) showed that clusters were present when 2.7-4 nm particles were detected. Kulmala et al. (2005a) showed the existence of clusters during a nucleation event but even more interestingly they showed that the clusters exist practically all the time. Recently, Kulmala et al. (2007a) observed the existence of neutral clusters and the initial state of atmospheric nucleation. However, due to the fact that measurements in sub-2 nm size range are challenging, more measurements, and preferably using different instruments, are needed to verify those observations.

Atmospheric aerosol formation is strongly coupled with chemistry, particularly with the formation of sulphuric acid and other vapours of very low volatility such as multi-functional organic compounds and iodine vapours (Curtius, 2006). Pre-existing aerosol particles, on the other hand, act as a sink for these vapours and nucleated clusters, thus inhibiting atmospheric aerosol formation. Aerosol formation seems to be related also to several meteorological parameters and phenomena, including the magnitude of solar radiation and atmospheric mixing processes such as the evolution of the continental boundary layer or the mixing of stratospheric and tropospheric air near the tropopause (Lyubovtseva et al., 2005).

In this paper we present the applicability of two condensation particle counter (CPC) systems to atmospheric molecular cluster measurements. We use those CPC systems in their improved status to observe quantitatively the concentration and size of atmospheric neutral clusters. The first CPC system is a modified TSI 3025A ultra-fine particle counter with white light optics (Marti et al., 1996; Dick et al., 2001) and the

**Atmospheric cluster
measurements**

M. Sipilä et al.

[Title Page](#)[Abstract](#)[Introduction](#)[Conclusions](#)[References](#)[Tables](#)[Figures](#)[◀](#)[▶](#)[◀](#)[▶](#)[Back](#)[Close](#)[Full Screen / Esc](#)[Printer-friendly Version](#)[Interactive Discussion](#)

second one is an adiabatic expansion type CPC (Kürten et al., 2005). We conducted also a set of laboratory tests with the CPC systems to assure their functionality to detect cluster sized objects. We also present atmospheric cluster concentration measured at a boreal forest site.

2 Condensation Particle Counter systems

The two used CPC systems were characterized with laboratory generated nanoparticles. A tungsten oxide generator (Grimm 7860, Grimm Aerosol Technik, GmbH) was used as a particle source down to mobility diameters of approximately 1.5 nm. Generated particles were charged by a radioactive Am-241 neutralizer (activity 60 MBq). A similar neutralizer was used also to generate ion clusters and neutral sub-2nm recombination clusters. A short (109 mm) Vienna type Differential Mobility Analyzer (DMA, Winklmayr et al., 1991) was used to classify the generated particles with a sheath flow of 20 lpm and aerosol flow from 1.5 to 2.5 lpm while a positive high voltage was applied to the DMA. A TSI-3068 electrometer was used as a reference for negatively charged clusters.

The CPC systems were also tested at atmospheric conditions. Field measurements were carried out during the EUCAARI (European Integrated project on Aerosol Cloud Climate and Air Quality Interactions) 2007 measurement campaign at the Hyytiälä field station (SMEAR II, Hari and Kulmala, 2005), southern Finland, from March to June 2007. This study focuses on measurements by a pulse height CPC and an expansion CPC, but utilizes also the supporting data from a Differential Mobility Particle Sizer DMPS (Aalto et al., 2001) and from a Balanced Scanning Mobility Analyzer, BSMA (Tammet 2004; 2006). The DMPS measures the particle size distributions from 3 nm up to 1 μm . The BSMA measures the ion mobility spectra in the mobility range of 3.2–0.032 $\text{cm}^2 \text{V}^{-1} \text{s}^{-1}$ which corresponds to the mobility equivalent diameter range of ca. 0.8–8 nm.

[Title Page](#)[Abstract](#)[Introduction](#)[Conclusions](#)[References](#)[Tables](#)[Figures](#)[◀](#)[▶](#)[◀](#)[▶](#)[Back](#)[Close](#)[Full Screen / Esc](#)[Printer-friendly Version](#)[Interactive Discussion](#)

2.1 Pulse Height Condensation Particle Counter (PH-CPC)

The first instrument, which applicability was investigated was the pulse height CPC. It exploits the axial gradient of butanol supersaturation inside the CPC condenser. Particles entering the condenser activate for growth at different axial positions depending on their size resulting in a monotonic link between initial particle size and final droplet size for initial particle sizes smaller than ca 15 nm (Saros et al., 1996). Scattering cross-section for white light is a monotonic function of droplet size. Therefore measuring the intensity of scattered light with a multi-channel analyzer (MCA) gives information about the initial particle size. This pulse height analysis method has been used in size distribution measurements between 3 and 10 nm (Weber et al., 1995, 1998) as well as to determine the composition of freshly nucleated nanoparticles (O'Dowd et al., 2002; Hanson et al., 2002).

The detection efficiency as a function of particle size in a conductive cooling type condensation particle counter is determined mainly by the particle transport efficiency from the inlet to the activation region inside the condenser, and by the saturation ratio of condensing vapour. The detection efficiency of commercial CPCs can be somewhat improved by increasing the supersaturation inside the condenser (see e.g. Mertes et al., 1995; Petäjä et al., 2006; Kulmala et al., 2007b). However, increasing the supersaturation too much induces homogeneous nucleation of the working fluid inside the condenser. This leads to excess counts in the optical detector due to homogeneously nucleated particles. This problem can be partly solved by application of pulse height analysis of the white light scattered by the droplets grown in the condenser (Saros et al., 1996).

We utilized the PH technique to distinguish between homogeneously formed butanol droplets and droplets formed by heterogeneous nucleation on molecular cluster sized objects inside the condenser. The PH-CPC used in this study is the TSI-3025A conductive cooling type CPC (Stolzenburg and McMurry, 1991) with modified optics (Dick et al., 2000) and a multi-channel analyzer. To maximize the activation probability of

Title Page

Abstract

Introduction

Conclusions

References

Tables

Figures

◀

▶

◀

▶

Back

Close

Full Screen / Esc

Printer-friendly Version

Interactive Discussion

the smallest clusters, the butanol supersaturation was increased by elevating the saturator temperature from normal 37°C up to 43–44°C and decreasing the condenser temperature by 0–2°C from nominal 10°C.

The concentration of particles entering the PH-CPC has an effect on the detection efficiency. According to Saros et al. (1996) the primary reason for this is dead time in the MCA. As more particles enter the system, there is not enough time for the MCA to recover from the previous signal. This leads to the dead-time, when neither pulse heights nor concentration can be measured. A secondary reason for the lowered detection efficiency of the PH-CPC in high concentrations is butanol vapour depletion. In high concentrations there are more particles competing for the same amount of vapour in the condenser. As a result, the particles reach smaller sizes and some of the smallest particles might not even activate. Thus, in larger than 4000 cm⁻³ aerosol number concentrations Saros et al. (1996) suggested a dilution system to be placed in front of the PH-CPC. This ensures that the MCA will have enough time to recover, the butanol is not depleted significantly and coincidence is minimal. To maximize the cluster concentration inside the PH-CPC condenser we conducted all measurements without dilution, as the typical background concentrations in Hyytiälä are below 4000 cm⁻³. Concentrations during nucleation event and pollution episodes, however, usually exceed 4000 cm⁻³ and therefore the data associating to these events of elevated concentration is not very reliable.

2.1.1 PH-CPC with a Diffusion Battery (DB) and an ion filter

Because the condensation sink formed by activated particles affects, besides the detection efficiency, also the homogeneous nucleation rate, we applied a diffusion battery (modified from TSI-3042) prior to the PH-CPC. This allowed us to determine the fraction of homogeneous nucleation in presence of larger, few nanometers and up, particles in the observed spectra. We used only four stages of the diffusion battery; the fourth stage was assumed to remove practically all cluster sized objects and the resulting distribution on the lower MCA channels is assumed to be due to homogeneous nucleation.

Atmospheric cluster measurements

M. Sipilä et al.

Title Page

Abstract

Introduction

Conclusions

References

Tables

Figures

◀

▶

◀

▶

Back

Close

Full Screen / Esc

Printer-friendly Version

Interactive Discussion

On the additional fifth stage, an absolute filter (HEPA, Pall Corporation) was used to remove all particles and molecular clusters, and in this case all detected pulses came from homogenous nucleation. Because of reasonably high losses already on the first stage of the diffusion battery, measurements with a free inlet were also conducted.

The particle penetration through the diffusion battery to the PH-CPC was characterized in the laboratory with the tungsten oxide generator and the DMA setup described above. The average size d_p of clusters (activated in the condenser) can be determined from

$$\Omega_{(i-j)/(k-l)}(d_p) = \frac{p_i(d_p) - p_j(d_p)}{p_k(d_p) - p_l(d_p)} = \frac{N_{\text{hom}} + N_i - (N_{\text{hom}} + N_j)}{N_{\text{hom}} + N_k - (N_{\text{hom}} + N_l)}, \quad (1)$$

where $\Omega_{(i-j)/(k-l)}(d_p)$ is an experimentally determined function which describes the relations of the different diffusion battery stages, $p_{i,j,k,l}(d_p)$ s are the penetrating fractions through the diffusion battery stages i, j, k and l as a function of particle diameter d_p , $N_{i,j,k,l}$ are the detected concentrations after the corresponding stages with signal from large particle activation subtracted, and N_{hom} is the signal due to homogeneous nucleation which is assumed to be constant during one diffusion battery cycle.

Charged ion clusters are present in variable concentrations in the atmosphere (e.g. Hirsikko et al. 2005; Kulmala and Tammet, 2007). In order to observe the signal due to the ion clusters, we applied an ion filter to the inlet of the PH-CPC. The ion filter was a 4 cm coaxial tube (i.d. 8 mm) with 32 V voltage between the electrodes. Electric field was switched on and off. The difference between the two PH-spectra revealed the concentration of ion clusters.

2.2 Expansion CPC

The second instrument to verify its applicability to atmospheric cluster measurements was an expansion CPC. In this instrument a rapid adiabatic expansion of gas-particle mixture leads to super-saturated conditions and subsequently activation of the particles as the super-saturated vapour condenses onto the sampled particles. A more detailed

[Title Page](#)
[Abstract](#)
[Introduction](#)
[Conclusions](#)
[References](#)
[Tables](#)
[Figures](#)
[◀](#)
[▶](#)
[◀](#)
[▶](#)
[Back](#)
[Close](#)
[Full Screen / Esc](#)
[Printer-friendly Version](#)
[Interactive Discussion](#)

discussion of the expansion technique can be found in Wagner (1985). The expansion CPC (E-CPC) used in this study was a modified version of the one described by Kürten et al. (2005). As the condensing vapour we used both water and butanol. Sample flow rate of the E-CPC was 2 l per min (lpm). A smaller flow (0.8 lpm) of particle free air saturated with the condensing vapour is mixed with the sample flow. This mixture is then directed to an expansion chamber. After the expansion, particles within the sample are activated and grow to sizes where they scatter visible light from the laser beam. In this instrument the amount of light forward-scattered ($1.1\text{--}4.4^\circ$) by the droplets inside the expansion chamber is measured as a function of time. Growing droplets scatter light depending on their size according to the Mie-theory and the concentration of droplets can be calculated from the scattering intensity maxima. We used the second Mie maximum for calculating the total number concentration of activated particles.

By scanning the expansion ratio (E) and thus changing the supersaturation inside the expansion chamber we were able to activate particles of different sizes. Expansion scans were performed with a free inlet and with a set of diffusion tubes. We used three parallel 4 mm inner diameter 1 m long copper tubes with a flow rate of ca. 0.7 lpm in each. The tubes have 50% penetration efficiency for 3.5 nm particles according to Gormley-Kennedy diffusion loss calculations (e.g. Baron and Willeke, 2001). Tube surfaces were assumed to be in equilibrium with the ambient water vapour concentration. These tubes were used to screen out the smallest clusters. In some measurements an ion filter similar to one used together with the PH-CPC was applied to detect the signal caused by the ion clusters.

To test the applicability of the E-CPC for atmospheric cluster measurements we generated ions and neutral recombination clusters with the Am-241 charger and the ion filter with water as the condensing vapour.

**Atmospheric cluster
measurements**

M. Sipilä et al.

Title Page

Abstract

Introduction

Conclusions

References

Tables

Figures

◀

▶

◀

▶

Back

Close

Full Screen / Esc

Printer-friendly Version

Interactive Discussion

3 Results

3.1 Laboratory experiments

3.1.1 Pulse height CPC in homogenous nucleation regime

As we increased the temperature difference between the saturator and the condenser of the PH-CPC, homogenous nucleation occurred inside the instrument. With negatively charged tungsten oxide particles we tested the limit where the droplets formed via heterogenous nucleation from the sampled particles could no longer be discriminated from the homogeneously nucleated butanol droplets. The resulting pulse-height spectra are presented in Fig. 1. Homogeneously nucleated droplets were clearly distinguishable from droplets nucleated heterogeneously on negatively charged WO_x calibration particles at least down to 2 nm.

Attached charge lowers the supersaturation needed for activation (Winkler et al., 2007). Therefore the results for negatively charged clusters are not necessarily representative of electrically neutral clusters. Unfortunately the generation of neutral sub-3 nm clusters of known composition, size and concentration is a very challenging task and therefore the complete laboratory verification of the effect of charge is left out of the scope of this study. However, to get an idea on where the pulses from ambient neutral sub-2nm clusters would appear, we generated neutral clusters by recombination of ions produced by radioactive decay. Inside an Am-241 source a vast amount of ions are generated. Some of these ions recombine and form electrically neutral stable clusters.

Without the electric filtration of the sample air a fraction of ions and neutral clusters formed in collisions between positive and negative ions were activated inside the PH-CPC. Total number concentration of activated clusters in this experiment was ca. 6000 cm^{-3} . When the ions were filtered away, the neutral clusters were clearly visible and distinguishable from homogeneous nucleation, even though their pulse height (PH) distribution partly overlaps with the PH-distribution of homogeneously nucleated

Title Page

Abstract

Introduction

Conclusions

References

Tables

Figures

◀

▶

◀

▶

Back

Close

Full Screen / Esc

Printer-friendly Version

Interactive Discussion

**Atmospheric cluster
measurements**

M. Sipilä et al.

Title Page

Abstract

Introduction

Conclusions

References

Tables

Figures

◀

▶

◀

▶

Back

Close

Full Screen / Esc

Printer-friendly Version

Interactive Discussion

droplets (Fig. 2). The PH-distribution of homogeneously nucleated droplets was determined by applying the diffusion tube to remove molecular clusters from the sample flow. This measurement was carried out with urban indoor air containing also aerosol particles, which were accumulating in the MCA channels 500–700. Also as a first indication of atmospheric neutral clusters, a shoulder was clearly seen in the Gaussian homogeneous nucleation spectra for just ambient unhandled sample (green line in Fig. 2). These indoor and urban air cluster measurements will not be discussed further here.

3.1.2 PH-CPC with a Diffusion Battery

An example of the diffusion battery function (1) is shown in Fig. 3. $\Omega_{(0-1)/(1-2)}$ approaches a value of unity when particle diameters are bigger than 3 nm. This shows that practically all bigger than 3 nm particles are penetrating through the diffusion battery stages 0-2. With particle sizes below 2 nm $\Omega_{(0-1)/(1-2)}$ increases rapidly showing that more and more particles are removed already on the stage 1. By determining $\Omega_{(0-1)/(1-2)}$ from the field data the corresponding cluster diameter can be obtained (see Sect. 3.2.).

3.1.3 Expansion CPC

In the laboratory tests with the Expansion CPC, water was used as the condensing vapour. The larger the expansion ratio, the smaller particles activate until the homogeneous nucleation of water vapour occurs. Kürten et al. (2005) have shown that the 50% cut-off size smaller than 3.5 nm can be achieved with the Expansion CPC. Here we have seen that even smaller particles can be detected with reasonably high efficiency.

To test the E-CPC for a polydisperse ambient aerosol population we varied the expansion ratio (E) from 1.4 to 2.5. Activation of background aerosol population occurred around E=1.5 and the onset of homogeneous nucleation was seen around E=2.3 (Fig. 4). Ions, however, as well as neutral clusters will activate well before that. We

tested the onset expansion ratios for Am-241 generated ion clusters by placing the radioactive neutralizer in front of the E-CPC. With this setup the onset took place at $E=1.9$. After filtering the ions the onset moved approximately up to $E=2.0$, which is close to the value where the onset for homogenous nucleation was observed with a diffusion tube.

Cluster concentration can be calculated by the differences in the measured concentrations with and without the diffusion tube and ion filter. Concentration of all activated clusters (charged and neutral) is the difference between the data obtained with the charger attached to the E-CPC and the concentration detected with the diffusion tube (base signal). A concentration of ca. $4 \times 10^4 \text{ cm}^{-3}$ is detected (Fig. 4). The concentration of neutral clusters, on the other hand, is the difference between readings with the charger - ion filter combination and the diffusion tube (ca. $2 \times 10^4 \text{ cm}^{-3}$). The concentration of ion clusters in this experiment is thus the difference between the total cluster concentration and neutral cluster concentration and it is of the order of $2 \times 10^4 \text{ cm}^{-3}$. Comparison of detected total cluster concentration ($\sim 4 \times 10^4 \text{ cm}^{-3}$) to corresponding signal detected by PH-CPC ($\sim 6000 \text{ cm}^{-3}$) show that detection efficiency of E-CPC is approximately 6–7 times higher than detection efficiency of PH-CPC for these clusters.

The reason why the measured concentrations bend down after the maximum in Fig. 4 is that activated clusters significantly consume condensing vapour when present at high concentrations. Thus homogeneous nucleation is prevented and the subtraction is not completely correct.

3.2 Ambient cluster concentrations

In order to find out their capability to detect atmospheric clusters both the Pulse-Height CPC and the Expansion CPC were deployed to a field campaign in Hyytiälä, Finland. Measurements were conducted between 1 March and 30 June 2007. PH-CPC, BSMA and DMPS were running throughout the whole campaign. E-CPC measurements were mainly carried out during May–June 2007. Out of those campaign days, three days were selected for a closer examination. One of the days was a new particle formation

Atmospheric cluster measurements

M. Sipilä et al.

Title Page

Abstract

Introduction

Conclusions

References

Tables

Figures

◀

▶

◀

▶

Back

Close

Full Screen / Esc

Printer-friendly Version

Interactive Discussion

event day (4 April 2007) and on two days (28 May and 12 June 2007) no newly formed particles were observed.

Data interpretation relating a specific MCA channel directly to a particle size is a complicated task. Channels in the pulse height spectra are drifting all the time due to e.g. changes in the intensity of white light source, total particle concentration, and small fluctuations in flows and temperatures. Because the pulse height also depends on the particle composition (O'Dowd et al., 2002), coupling the channels to particle sizes becomes even more difficult. Another difficulty is the determination of the absolute concentration of sub-3nm particles from the data, since the supersaturation and thus the activation probability strongly depends on the continuously changing ambient total particle concentration. Therefore these results are still somewhat qualitative. However, order of magnitude estimates can be given.

The calibration of the instrument for neutral sub-2nm particles and clusters is practically a very challenging task as there is no reference instrument and due to the unknown composition of ambient clusters. Therefore, to get an estimation for the neutral cluster detection efficiency we investigated the detection efficiency of the PH-CPC for atmospheric ion clusters. The detection efficiency was obtained by switching the ion trap electric field on and off and comparing the ion cluster concentration detected by the PH-CPC to the ion cluster concentration measured by the BSMA. This gives the highest estimation for the detection efficiency of neutral clusters under the assumption that neutral cluster activation probability does not exceed the ion activation probability. However, the ion cluster detection efficiency fluctuated considerably due to changes in supersaturation inside the condenser. The highest measured detection efficiencies for ion clusters were approximately 3% whereas the lowest records were buried in the noise, being practically 0%. The typical size of negatively charged cluster ions according to BSMA was 0.7–1.4 nm, positive ones being slightly larger from 1 up to ca. 1.6 nm (mobility equivalent diameter). To get an accurate estimation for the neutral cluster detection efficiency the efficiency for ions should have been recorded continuously. Therefore the most reliable data are associated to ion detection efficiency

**Atmospheric cluster
measurements**

M. Sipilä et al.

[Title Page](#)[Abstract](#)[Introduction](#)[Conclusions](#)[References](#)[Tables](#)[Figures](#)[I◀](#)[▶I](#)[◀](#)[▶](#)[Back](#)[Close](#)[Full Screen / Esc](#)[Printer-friendly Version](#)[Interactive Discussion](#)

measurements, and the three example days are presented below.

3.2.1 Particle formation event day

On 4 April 2007 new particle formation occurred in Hyytiälä. Few hours after the sunrise a new mode of atmospheric particles was detected with a Differential Mobility Particle Sizer (DMPS), which has a lower detection limit of 3 nm. Meanwhile the total number concentration increased by an order of magnitude from 10^3 to 10^4 cm^{-3} (Fig. 5).

Taking a closer look on the PH-spectra revealed that the first steps of nucleation are recorded with the PH-CPC. Figure 6 shows the development of PH spectrum during an event day as a series of snapshots taken at 06:00, 08:00, 10:30 and 11:00 local time.

Throughout the day there was a clear bimodal distribution on the lower MCA channels and a dominating peak at higher channels. Lower channels around 200–300 represent homogeneously formed butanol droplets and the largest peak at around 700–800 is the signal from ambient aerosol particles larger than ~ 10 nm in size. The droplet concentration due to homogeneous nucleation was measured using the diffusion battery from time to time and outside these times we relied on the symmetry of the pulse height spectrum of pure homogeneous butanol nucleation. Subtracting the maximum possible concentration from homogeneous nucleation leaves a residual mode in channels from 300 to 500. The pulse count in this residual mode before and after the nucleation event corresponds to ambient concentration of 40–100 cm^{-3} if the detection efficiency is not accounted for. If the detection efficiency of 2% is assumed (see next section for discussion on the detection efficiency), ambient concentration of 2000–5000 cm^{-3} is needed to explain the observed signal.

At 09:00 (Fig. 6b) over an hour before new particle formation is detected with the DMPS (ca. 10:15), the particles start to appear between the MCA channels 400–600. When the event starts to be visible in the DMPS, homogeneous nucleation disappears rapidly from the PH spectrum due to the increasing particle concentration and subsequent depletion of butanol vapour. Hence, also the activation probability of the smallest clusters decreases and the detection efficiency drops.

Title Page

Abstract

Introduction

Conclusions

References

Tables

Figures

◀

▶

◀

▶

Back

Close

Full Screen / Esc

Printer-friendly Version

Interactive Discussion

[Title Page](#)[Abstract](#)[Introduction](#)[Conclusions](#)[References](#)[Tables](#)[Figures](#)[◀](#)[▶](#)[◀](#)[▶](#)[Back](#)[Close](#)[Full Screen / Esc](#)[Printer-friendly Version](#)[Interactive Discussion](#)

The laboratory and field measurements with the diffusion battery both showed that homomolecular homogeneous nucleation always appeared as a Gaussian shaped pulse count distribution in the PH spectra (Fig. 1). Data, however, typically showed a clear bimodal distribution (Fig. 6a) between the MCA channels 100–500 throughout the several months measurement period even though (and especially when), according to DMPS, no particles between 3 nm and 10 nm were present. Also, laboratory tests showed that co-incidence would not occur with that level of homogeneous nucleation. This fact proves that besides homomolecular butanol nucleation and large particle activation, a third process takes place in the supersaturated butanol aerosol mixture.

3.2.2 Non event days

28 May 2007

Figure 7 shows one experiment from 28 May 2007 where measurements were conducted with the free inlet (blue curve), with the ion filter (black curve), and with the all clusters removing diffusion tube (red curve, 50%-cut-off at 3.5 nm). Ion cluster detection efficiency is ca 3% in this case from the comparison to the BSMA (1100 cm^{-3}). Using this, the total cluster concentration here would be at least 5200 cm^{-3} . Notably, the level of homogeneous nucleation (red curve, this measurement is conducted in lower supersaturation than the experiment presented in Fig. 6) is reasonably low compared to signal from activating clusters, indicating that increasing the supersaturation after the onset of homogeneous nucleation in presence of background aerosol does not anymore amend the detection efficiency significantly, but the nanoparticle transport losses from the inlet to the condenser start to dominate.

Besides large fluctuations in the detected signal, also the average size, determined from diffusion battery measurements using equation 1 showed quite unstable behaviour. Average signal ratio $\Omega_{(0-1)/(1-2)}$ for June was 1.774 with standard deviation of 0.789 which corresponds to an average cluster mobility diameter of approximately

**Atmospheric cluster
measurements**

M. Sipilä et al.

Title Page

Abstract

Introduction

Conclusions

References

Tables

Figures

◀

▶

◀

▶

Back

Close

Full Screen / Esc

Printer-friendly Version

Interactive Discussion

1.8 nm (see Fig. 3). As a comparison, measurement with artificial charger generated neutral recombination clusters yielded $\Omega_{(0-1)/(1-2)}=1.60$ which corresponds to the mobility diameter of 1.9 nm. From the standard deviation of $\Omega_{(0-1)/(1-2)}$ we get an lower end error estimation for the diameter to be ca. 1.6 nm. Using standard deviation of $\Omega_{(0-1)/(1-2)}$ no realistic estimation for the upper limit of particle size can be obtained, but it is clear from the pulse height spectra and the supporting data that the clusters observed during non-event times have to be smaller than 3 nm in diameter. Besides the relatively large scattering of $\Omega_{(0-1)/(1-2)}$, also the error arising from diffusion battery calibration inaccuracy is obviously quite high with such small particle sizes. Furthermore, it should be emphasized that the determined diameter of ca. 1.8 nm is the average size of the detected clusters, and is not necessarily equal to the true average size of the whole cluster pool. The counting efficiency of the PH-CPC can be strongly enhanced for the largest clusters. Therefore the 1.8 nm given here should be taken only as suggestive.

Two examples from E-CPC measurements are presented in Figs. 8 and 9. Expansion scans with water and butanol as the working fluid both yielded qualitatively the same results. Unfortunately with the current setup the simultaneous measurement with butanol and water was not possible and therefore no indication of e.g. solubility or composition of these clusters can be obtained from the data.

Large particles activate first after which there is a plateau in the concentration curve (Figs. 8 and 9). Finally, concentration starts to increase rapidly. The difference between the experiments where cluster-sized objects were present, or removed by the diffusion tubes (see Sect. 2.2) is clear. The concentration difference between these two curves around the onset of homogeneous nucleation gives directly the concentration of clusters activated inside the expansion chamber. The signal is rapidly covered by the fluctuations when the concentration starts to increase. Nucleation rate is highly sensitive to several parameters, such as temperature and saturation ratio which are not controlled in high enough accuracy. That causes the large fluctuations after homogeneous nucleation starts.

**Atmospheric cluster
measurements**

M. Sipilä et al.

[Title Page](#)[Abstract](#)[Introduction](#)[Conclusions](#)[References](#)[Tables](#)[Figures](#)[◀](#)[▶](#)[◀](#)[▶](#)[Back](#)[Close](#)[Full Screen / Esc](#)[Printer-friendly Version](#)[Interactive Discussion](#)

It is noteworthy that the activation of clusters takes place at the same expansion ratios as the activation of laboratory generated recombination clusters (Fig. 4). This supports the assumption that the observed signal really is due to the cluster activation and not e.g. multicomponent homogeneous nucleation.

5 Few experiments with the ion filter at the inlet were conducted but the high fluctuations covered the possible signal from the ion activation. This was expected, since close to the onset of homogeneous nucleation the fluctuations, or noise, in the signal were typically $\sim 1000 \text{ cm}^{-3}$. Assuming e.g. 5–10% detection efficiency for ions would lead to signals by a factor of 5–10 smaller than the noise level with the typical cluster ion concentrations ($\sim 2000 \text{ cm}^{-3}$). Thus, extracting the ion signal from this limited data set was not possible.

12 June 2007

15 Before any indication of new particle formation was observed by the DMPS, the PH-CPC detected clusters at sizes below the detection limit of the DMPS (Fig. 6). Another example of the detected cluster pool is shown in Fig. 10. Data is recorded during a non-event day on 12 June 2007. The figure shows the difference in signals measured with the diffusion battery stages 0 and 3. Detection efficiency or losses on the zeroth stage are not accounted for. Throughout the day a clear signal around channel 300 was observed suggesting continuous presence of clusters. Larger particles (not affected by the diffusion battery) are once again accumulating in channels around 600.

25 Figure 11 shows the total cluster concentrations measured by the PH-CPC and the E-CPC, and ion cluster concentration measured by the BSMA on 12 June 2007 (same day as in Fig. 10). For PH-CPC a detection efficiency of 2% and diffusion battery 0-stage penetration of 40% (1.8 nm particles) is assumed. The detection efficiency of the E-CPC for the artificial charger generated clusters was 6–7 times higher than the corresponding efficiency of the PH-CPC. Detection efficiency was within the measurement

**Atmospheric cluster
measurements**

M. Sipilä et al.

[Title Page](#)[Abstract](#)[Introduction](#)[Conclusions](#)[References](#)[Tables](#)[Figures](#)[◀](#)[▶](#)[◀](#)[▶](#)[Back](#)[Close](#)[Full Screen / Esc](#)[Printer-friendly Version](#)[Interactive Discussion](#)

accuracy independent of the working fluid indicating that the detection efficiency of the E-CPC with the scanning technique is mainly determined by the nanoparticle transport losses from the inlet to the expansion chamber rather than the activation probability. Therefore a detection efficiency of 13% was assumed for the E-CPC for both working fluids used. It should be emphasized that these are only rough estimates and the true detection efficiencies can be significantly different. However, it is clearly seen in Fig. 11 that the order of magnitude is the same in both PH-CPC and E-CPC measurements. Similarities in diurnal behaviour between the total cluster concentration detected by the PH-CPC and the ion cluster concentration can be seen. However, the variation in total cluster concentration is much higher than in the ion cluster concentration.

4 Discussion

Both pulse height and expansion CPC measurements showed that besides the large (>3 nm) particle activation and the homogeneous self-nucleation of the working fluid, there is a third process taking place in the supersaturated conditions inside the PH-CPC condenser and the E-CPC expansion chamber. This process was concluded to be most likely neutral cluster activation (see also Kulmala et al., 2006, 2007a, 2007b). Several factors provide evidence in favour of this process. First, ion clusters alone cannot explain the observed signal as shown for example in Fig. 7. Second, the size of the clusters determined from diffusion battery measurements was reasonably large, around 1.8 nm in mobility equivalent diameter. Such a size would correspond to an object with a mass of approximately 1000 amu (Kilpatrick, 1971; Mäkelä et al., 1996). Such a mass could, in principle, be exceeded by large organic molecules. It means that with the current measurement setup we are approaching molecular sizes in nanoparticle detection.

The data does not directly show that the observed (neutral) clusters were thermodynamically stable (Kulmala, et al., 2000; Vehkamäki, 2004). However, since the composition of surrounding gas changes when the clusters enter the PH-CPC condenser

**Atmospheric cluster
measurements**

M. Sipilä et al.

[Title Page](#)[Abstract](#)[Introduction](#)[Conclusions](#)[References](#)[Tables](#)[Figures](#)[◀](#)[▶](#)[◀](#)[▶](#)[Back](#)[Close](#)[Full Screen / Esc](#)[Printer-friendly Version](#)[Interactive Discussion](#)

(90% of the sample air is filtered and saturated with butanol vapour before it is directed to the condenser), it is reasonable to assume that they were at least to some extent stable or slowly growing dynamic clusters. The survival probability of unstable clusters from the inlet to the point of activation should be rather poor. Also, since similar concentrations were detected with two instruments with different design and operation principle, it would be very surprising if the survival probabilities of unstable weakly bonded clusters were equal in both instruments.

If the observed signal is due to cluster activation inside the CPC, can we then conclude something about the formation mechanism of these clusters? The diurnal trend in cluster concentration measured with the PH-CPC correlates somewhat with the ion concentration measured by the BSMA. This is partly due to the fact that the neutral and the ion cluster concentrations should both be dependent on the coagulation sink provided by larger aerosol particles. From Fig. 11 it seems that the cluster concentration is higher during night time indicating that the source of neutral clusters is stronger on the surface layer since, after the boundary layer mixing in the morning the concentration goes down. This observation suggests that the cluster formation rate is dependent either on atmospheric ion concentration, which is higher during night-time because of an elevated radon level, or biological activities. However, because of numerous uncertainties influencing the PH-CPC detection efficiency, this observation is still very uncertain.

Ion-ion recombination is also expected to form stable clusters. Kulmala et al. (2007a), however, showed that the concentration of clusters formed by recombination is typically from few tens to few hundreds cm^{-3} , while our estimation for typical neutral cluster concentrations were from some thousands up to few tens of thousands. Thus also other cluster formation pathways possibly involving organic chemistry are needed.

5 Conclusions

We have investigated the applicability of two different CPC systems on atmospheric cluster detection, and in practise we were able to detect atmospheric sub-2 nm clusters using a PH-CPC and an E-CPC. Since the existence of those clusters have been observed very recently (Kulmala et al., 2007a) more measurements with different instruments were inquired to ensure their existence and also quantify their size and concentration. Using both instruments we were able to verify the existence of neutral clusters and also that we are able to observe them continuously. Besides this the observed size and concentrations give similar (not identical) numbers using both instruments. The observed cluster size was around 1.5–2 nm in mobility equivalent diameter. The concentration of clusters was typically ca. 5–10 times higher than the ion cluster concentration and also 2–5 times higher than the concentration of the sum of ion clusters and recombination clusters. Therefore a pool of neutral clusters seems to exist in the boreal forest environment and these results support our recent results (Kulmala et al., 2007a).

The measured cluster concentrations are still uncertain and more detailed investigations are needed to improve the instruments, and to accurately calibrate and test them. In any case we can consider the values given here as lower limits of the cluster concentration, since we were most probably not able to observe neutral clusters with sizes approaching 1 nm.

The origin of the observed clusters is still open. They can be thermodynamically stable clusters like ammonium bisulphate clusters proposed by Vehkamäki et al. (2004) or they can be slowly growing dynamic clusters. Some part could even be “snapshot clusters” forming and decaying dynamically and existing only shortly during observation. However, those clusters are supposed to activate (e.g. Kulmala et al., 2006) probably with sulphuric acid. The main mechanism for atmospheric nucleation would then be the activation of the more or less permanently existing clusters. Since the activation mechanism is easy to parameterize (Spracklen et al., 2006), it means that the

Atmospheric cluster measurements

M. Sipilä et al.

Title Page

Abstract

Introduction

Conclusions

References

Tables

Figures

◀

▶

◀

▶

Back

Close

Full Screen / Esc

Printer-friendly Version

Interactive Discussion

atmospheric nucleation can be used in large scale aerosol models without doubt.

Acknowledgements. This work has been partially funded by European Commission 6th Framework programme project EUCAARI, contract no 036833-2 (EUCAARI). Maj and Tor Nessling foundation is acknowledged for financial support.

References

- Aalto, P., Hämeri, K., Becker, E., Weber, R., Salm, J., Mäkelä, J. M., Hoell, C., O'Dowd, C. D., Karlsson, H., Hansson, H.-C., Väkevää, M., Koponen, I. K., Buzorius, G., and Kulmala, M.: Physical characterization of aerosol particles in boreal forests, *Tellus B*, 53, 344–358, 2001.
- Baron, P. A. and Willeke, K. (Eds.): *Aerosol Measurement – Principles, Techniques, and Applications*, 2nd edition, John Wiley and Sons, New York, 1131 pp., 2001.
- Curtius, J.: Nucleation of Atmospheric Aerosol Particles, *C. R. Phys.*, 7, 1027–1045, 2006.
- Dick, W. D., McMurry, P. H., Weber, R. J., and Quant, R.: White-light detection for nanoparticle sizing with the TSI Ultrafine Condensation Particle Counter, *J. Nanopart. Res.*, 2, 85–90, 2000.
- Hanson, D. R., Eisele, F. L., Ball, S. M., and McMurry, P. M.: Sizing small sulfuric acid particles with an ultrafine particle condensation nucleus counter, *Aerosol Sci. Tech.*, 36, 554–559, 2002.
- Hari, P. and Kulmala, M.: Station for measuring ecosystem-atmosphere relations (SMEAR II), *Boreal Environ. Res.*, 10, 315–322, 2005.
- Kerminen, V.-M., Pirjola, L., and Kulmala M.: How significantly does coagulation scavenging limit atmospheric particle production?, *J. Geophys. Res.*, 106, 24, 119–126, 2001.
- Kilpatrick, W. D.: An experimental mass-mobility relation for ions in air at atmospheric pressure, *Proc. Annu. Conf. Mass Spectrosc.*, 19, 320–325, 1971.
- Kulmala, M., Pirjola, L., and Mäkelä, J. M.: Stable sulphate clusters as a source of new atmospheric particles, *Nature*, 404, 66–69, 2000.
- Kulmala, M.: How particles nucleate and grow?, *Science*, 302, 1000–1001, 2003.
- Kulmala, M., Vehkamäki, H., Petäjä, T., Dal Maso, M., Lauri, A., Kerminen, V.-M., Birmili, W., and McMurry, P. H.: Formation and growth rates of ultrafine atmospheric particles: a review of observations, *J. Aerosol Sci.*, 35, 143–176, 2004.

Atmospheric cluster measurements

M. Sipilä et al.

Title Page

Abstract

Introduction

Conclusions

References

Tables

Figures

◀

▶

◀

▶

Back

Close

Full Screen / Esc

Printer-friendly Version

Interactive Discussion

**Atmospheric cluster
measurements**

M. Sipilä et al.

Title Page

Abstract

Introduction

Conclusions

References

Tables

Figures

◀

▶

◀

▶

Back

Close

Full Screen / Esc

Printer-friendly Version

Interactive Discussion

- Kulmala M., Lehtinen K. E. J., Laakso, L., Mordas, G., and Hämeri, K.: On the existence of neutral atmospheric clusters, *Boreal Environ. Res.*, 10, 79–87, 2005.
- Kulmala, M., Lehtinen, K. E. J., and Laaksonen, A.: Cluster activation theory as an explanation of the linear dependence between formation rate of 3 nm particles and sulphuric acid concentration, *Atmos. Chem. Phys.*, 6, 787–793, 2006,
5 <http://www.atmos-chem-phys.net/6/787/2006/>.
- Kulmala, M., and Tammet, H.: Finnish-Estonian air ion and aerosol workshops, *Boreal Env. Res.* 12, 237-245, 2007.
- Kulmala, M., Riipinen, I., Sipilä, M., Manninen, H., Petäjä, T., Junninen H., Dal Maso, M., Mordas, G., Mirme, A., Vana, M., Hirsikko, A., Laakso, L., Harrison, R. M., Hanson, I., Leung, C., Lehtinen, K. E. J., and Kerminen, V.-M.: Towards direct measurement of atmospheric nucleation, *Science*, 318, 89–92, 2007a.
- Kulmala, M., Mordas, G., Petäjä, T., Grönholm, T., Aalto, P. P., Vehkamäki, H., Hienola, A. I., Herrmann, E., Sipilä, M., Riipinen, I., Manninen, H. E., Hämeri, K., Stratmann, F., Bilde, M., Winkler, P. M., Birmile, W., and Wagner, P. E.: The condensation particle counter battery (CPCB): A new tool to investigate the activation properties of nanoparticles, *J. Aerosol Sci.*, 38, 289–304, 2007b.
- Kürten, A., Curtius, J., Nillius, B., and Borrmann, S.: Characterization of an automated, water-based expansion condensation nucleus counter for ultrafine particles, *Aerosol Sci. Tech.*, 39, 1174–1183, 2005.
- Lyubovtseva, Y. S., Sogacheva, L., Dal Maso, M., Bonn, B., Keronen, P., and Kulmala, M.: Seasonal variations of trace gases, meteorological parameters, and formation of aerosols in boreal forests, *Boreal Environ. Res.*, 10, 493–510, 2005.
- Marti, J. J., Weber, R. J., Saros, M. T., Vasilou, J. G., and McMurry, P. H.: Modification of the TSI 3025 Condensation Particle Counter for pulse height analysis, *Aerosol Sci. Tech.*, 25, 214–218, 1996.
- Mertes, S., Schröder, F., and Wiedensohler, A.: The particle detection efficiency curve of the TSI-3010 CPC as a function of temperature difference between saturator and condenser, *Aerosol Sci. Tech.*, 23, 257–261, 1995.
- Mäkelä, J. M., Jokinen, V., Mattila, T., Ukkonen, A., and Keskinen, J.: Mobility distribution of acetone cluster ions, *J. Aerosol Sci.*, 27, 175–190, 1996.
- O'Dowd, C. D., Aalto, P., Hämeri, K., Kulmala, M., and Hoffmann, T.: Atmospheric particles from organic vapours, *Nature*, 416, 497–498, 2002.

**Atmospheric cluster
measurements**

M. Sipilä et al.

Title Page

Abstract

Introduction

Conclusions

References

Tables

Figures

◀

▶

◀

▶

Back

Close

Full Screen / Esc

Printer-friendly Version

Interactive Discussion

Saros, M., Weber, R. J., Marti, J., and McMurry, P. H.: Ultra fine aerosol measurement using a condensation nucleus counter with pulse height analysis, *Aerosol Sci. Tech.*, 25, 200–213, 1996.

Spracklen, D. V., Carslaw, K. S., Kulmala, M., Kerminen, V.-M., Mann, G. W., and Sihto, S.-L.: The contribution of boundary layer nucleation events to total particle concentrations on regional and global scales, *Atmos. Chem. Phys.*, 6, 5631–5648, 2006,
<http://www.atmos-chem-phys.net/6/5631/2006/>.

Stoltzenburg, M. R. and McMurry, P. H.: An ultrafine aerosol condensation nucleus counter, *Aerosol Sci. Tech.*, 14, 48–65, 1991.

Tammet, H.: Balanced scanning mobility analyzer BSMA, in: *Nucleation and atmospheric aerosols 2004*, edited by: Kasahara, M. and Kulmala, M., 16th International Conference, Kyoto University Press, Japan, 294–297, 2004.

Tammet, H. and Kulmala, M.: Simulation tool for atmospheric aerosol nucleation bursts, *J. Aerosol Sci.*, 36, 173–196, 2005.

Tammet, H.: Continuous scanning of the mobility and size distribution of charged clusters and nanometer particles in atmospheric air and the balanced scanning mobility analyzer BSMA, *Atmos. Res.*, 82, 523–535, 2006.

Vehkamäki, H., Napari, I., Kulmala, M. and Noppel, M.: Stable ammonium bisulphate clusters in the atmosphere, *Phys. Rev. Lett.* 93, 148 501, doi:10.1103/PhysRevLett.93.14850, 2004.

Wagner, P. E.: A constant-angle Mie scattering method (CAM) for investigation of particle formation processes, *J. Colloid Interf. Sci.*, 105, 456–467, 1985.

Weber, R. J., McMurry, P. H., Eisele, F. L., and Tanner, D. J.: Measurement of expected nucleation precursor species and 3-500-nm diameter particles at Mauna Loa observatory, Hawaii, *J. Atmos. Sci.*, 52, 2242–2257, 1995.

Weber, R. J., Stolzenburg, M. R., Pandis, S. N., and McMurry, P. H.: Inversion of ultrafine condensation nucleus counter pulse height distributions to obtain nanoparticle (~3–10 nm) size distributions, *J. Aerosol Sci.*, 29, 601–615, 1998.

Winkler, P. M., Steiner, G. W., Reischl, G. P., Vrtala, A., Wagner, P. E., and Kulmala, M.: The effect of seed particle charge on heterogeneous nucleation, in: *Nucleation and atmospheric aerosols 2007*, edited by: O'Dowd, C. D. and Wagner P. E., 17th International Conference, Springer, 358–362, 2007.

Atmospheric cluster
measurements

M. Sipilä et al.

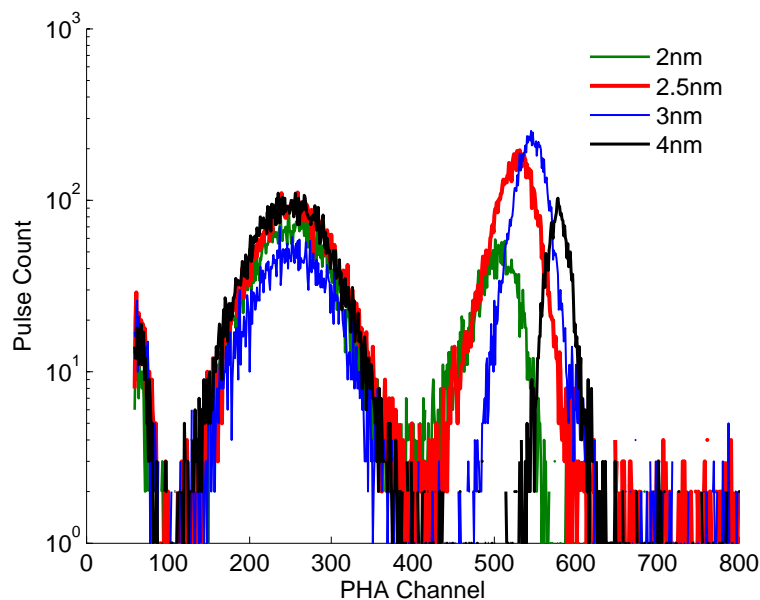


Fig. 1. Pulse height spectra for different sizes of WO_x particles. Homogenous nucleation appears as Gaussian shaped PH-spectrum between the channels ~ 100 and 400. Activated WO_x particles are seen in the channels 400–600. Larger initial particles yield higher pulses. Pulse count is the total number of pulses counted during the integration time (here 45 s), and can be taken as an arbitrary unit.

[Title Page](#)[Abstract](#)[Introduction](#)[Conclusions](#)[References](#)[Tables](#)[Figures](#)[◀](#)[▶](#)[◀](#)[▶](#)[Back](#)[Close](#)[Full Screen / Esc](#)[Printer-friendly Version](#)[Interactive Discussion](#)

EGU

Atmospheric cluster
measurements

M. Sipilä et al.

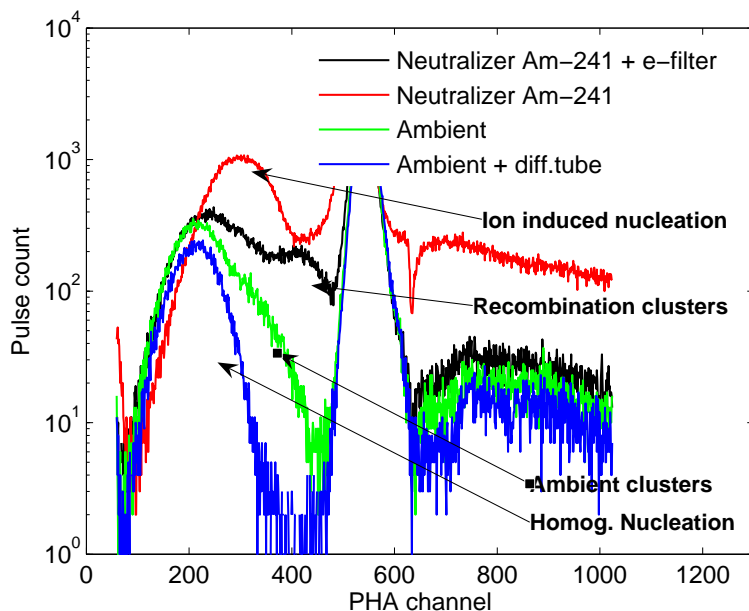


Fig. 2. Pulse height spectra from ambient indoor air (green line), ambient indoor air pre-treated by removing clusters by use of a diffusion tube (blue), by adding bipolar ions generated in an Am^{241} -source (red), and by adding neutral recombination clusters (black).

[Title Page](#)[Abstract](#)[Introduction](#)[Conclusions](#)[References](#)[Tables](#)[Figures](#)[◀](#)[▶](#)[◀](#)[▶](#)[Back](#)[Close](#)[Full Screen / Esc](#)[Printer-friendly Version](#)[Interactive Discussion](#)

EGU

Atmospheric cluster
measurements

M. Sipilä et al.

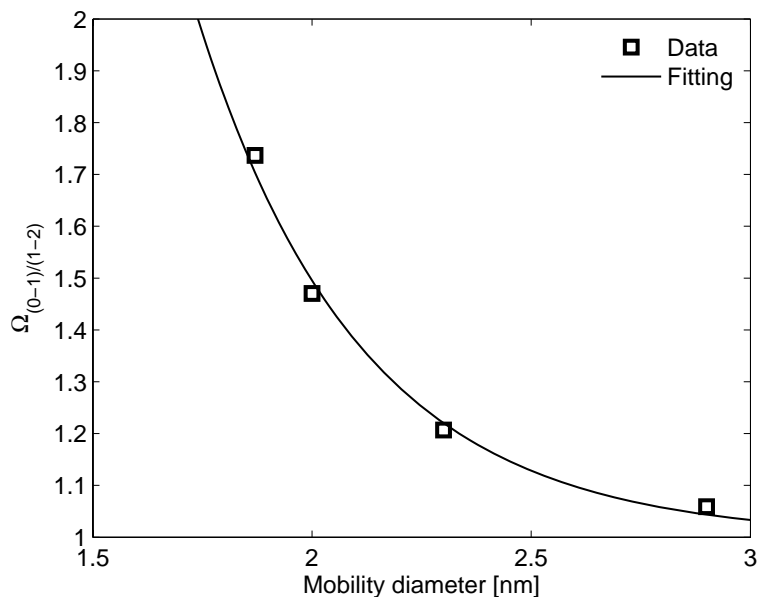


Fig. 3. Experimentally determined diffusion battery function (see Eq. (1)) describing the relations of stages 0, 1 and 2. $\Omega_{(0-1)/(1-2)}$ can be obtained from the field data and the average diameter solved using this function.

[Title Page](#)[Abstract](#)[Introduction](#)[Conclusions](#)[References](#)[Tables](#)[Figures](#)[◀](#)[▶](#)[◀](#)[▶](#)[Back](#)[Close](#)[Full Screen / Esc](#)[Printer-friendly Version](#)[Interactive Discussion](#)

EGU

Atmospheric cluster
measurements

M. Sipilä et al.

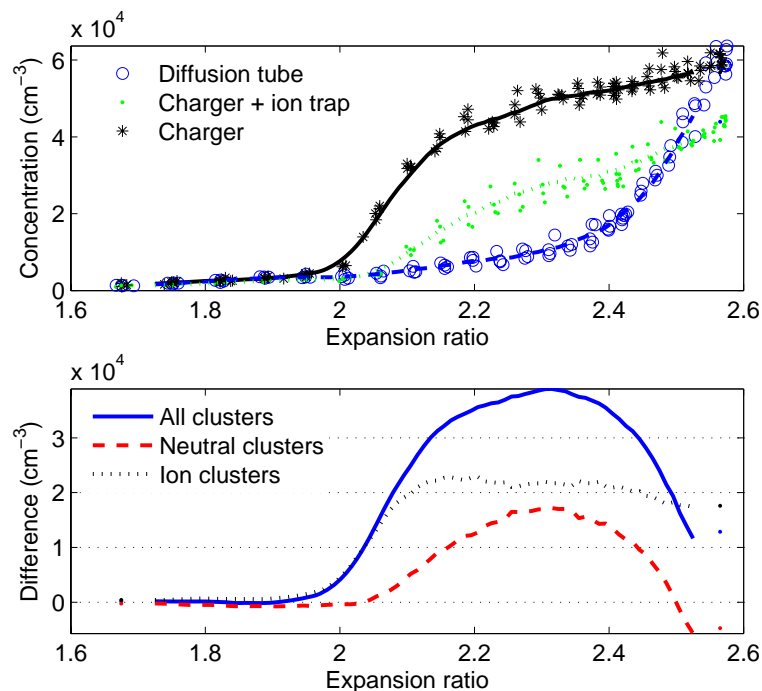


Fig. 4. Expansion scan experiment using bipolar ions generated in Am^{241} -source, and neutral recombination clusters. Measurement was carried out in ambient indoor air with water as condensing vapour. A diffusion tube was used to remove also natural clusters from the sample. Upper figure shows the detected signals. Concentration resulting from the subtraction of the signals is presented in lower figure.

[Title Page](#)[Abstract](#)[Introduction](#)[Conclusions](#)[References](#)[Tables](#)[Figures](#)[◀](#)[▶](#)[◀](#)[▶](#)[Back](#)[Close](#)[Full Screen / Esc](#)[Printer-friendly Version](#)[Interactive Discussion](#)

EGU

Atmospheric cluster
measurements

M. Sipilä et al.

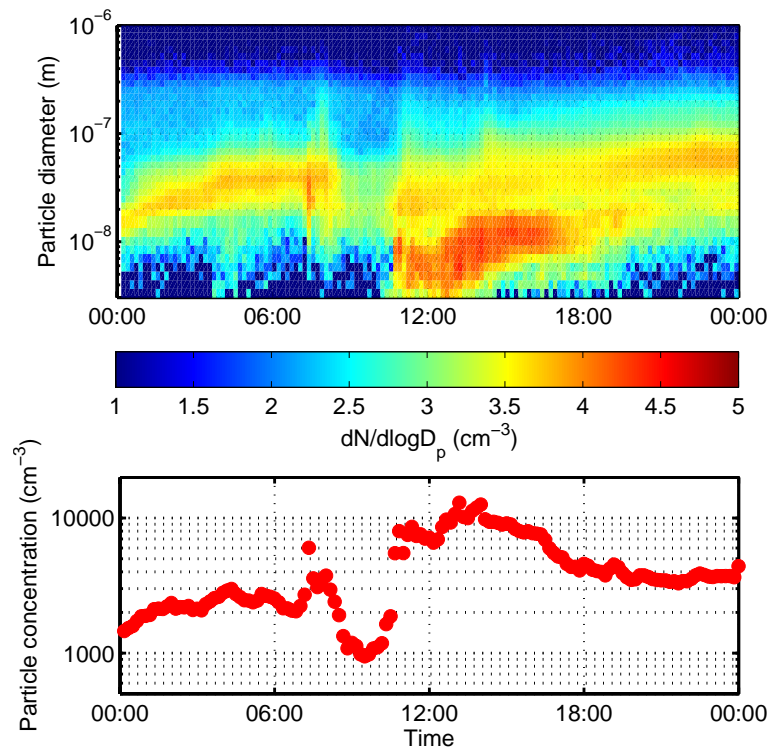


Fig. 5. Nucleation event on 4 April 2007 recorded by the DMPS.

[Title Page](#)[Abstract](#)[Introduction](#)[Conclusions](#)[References](#)[Tables](#)[Figures](#)[I◀](#)[▶I](#)[◀](#)[▶](#)[Back](#)[Close](#)[Full Screen / Esc](#)[Printer-friendly Version](#)[Interactive Discussion](#)

EGU

Atmospheric cluster
measurements

M. Sipilä et al.

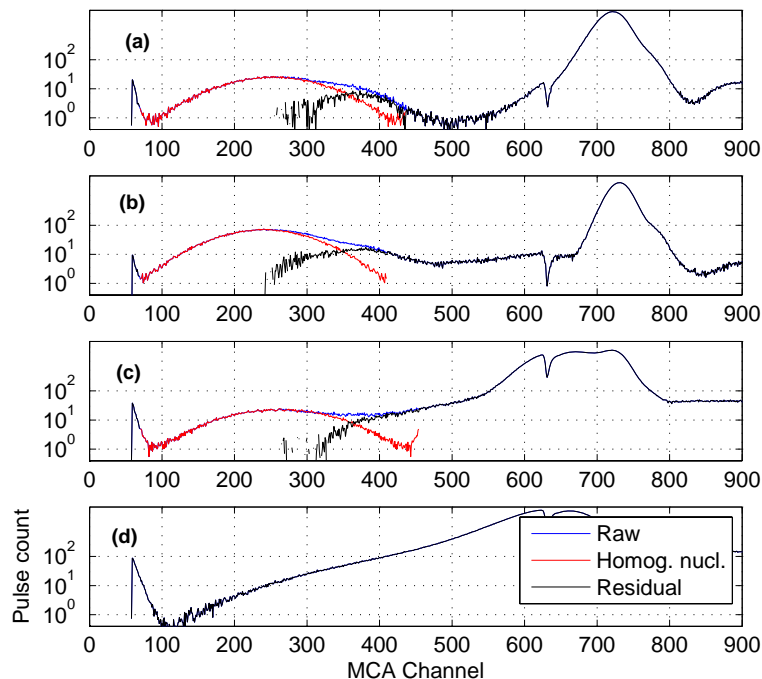


Fig. 6. Pulse height spectra recorded during an event day (4 April 2007) at 06:00 (a), 09:00 (b), 10:30 (c) and 11:00 (d). Blue line shows the raw-data, red line represents the PH-spectrum from homogeneous nucleation and black line describes the PH-spectrum after subtraction of homogeneous nucleation. The cluster mode is seen in channels between 300 and 500 (a). Large particles are accumulating in the channels 600–800. Approximately an hour before the beginning of the nucleation event is recorded by DMPS (see Fig. 5) freshly nucleated particles start to appear between the channels 400 and 600 (b). The increasing number concentration decreases the supersaturation most probably affecting the detection efficiency (c)–(d).

[Title Page](#)[Abstract](#)[Introduction](#)[Conclusions](#)[References](#)[Tables](#)[Figures](#)[◀](#)[▶](#)[◀](#)[▶](#)[Back](#)[Close](#)[Full Screen / Esc](#)[Printer-friendly Version](#)[Interactive Discussion](#)

EGU

Atmospheric cluster
measurements

M. Sipilä et al.

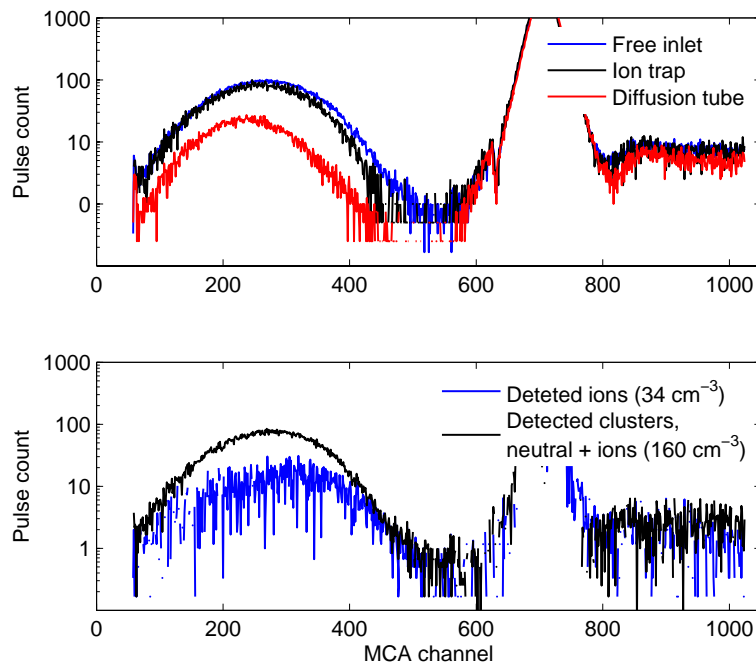


Fig. 7. (a) Example of pulse height distribution measured on 28 May 2007 with the free inlet (blue), with an ion filter (black) and with a diffusion tube (red) on the inlet. (b) Resulting distributions after subtracting the ion filter data (blue) and the diffusion tube data (black) from the free inlet data.

[Title Page](#)[Abstract](#)[Introduction](#)[Conclusions](#)[References](#)[Tables](#)[Figures](#)[◀](#)[▶](#)[◀](#)[▶](#)[Back](#)[Close](#)[Full Screen / Esc](#)[Printer-friendly Version](#)[Interactive Discussion](#)

EGU

Atmospheric cluster
measurements

M. Sipilä et al.

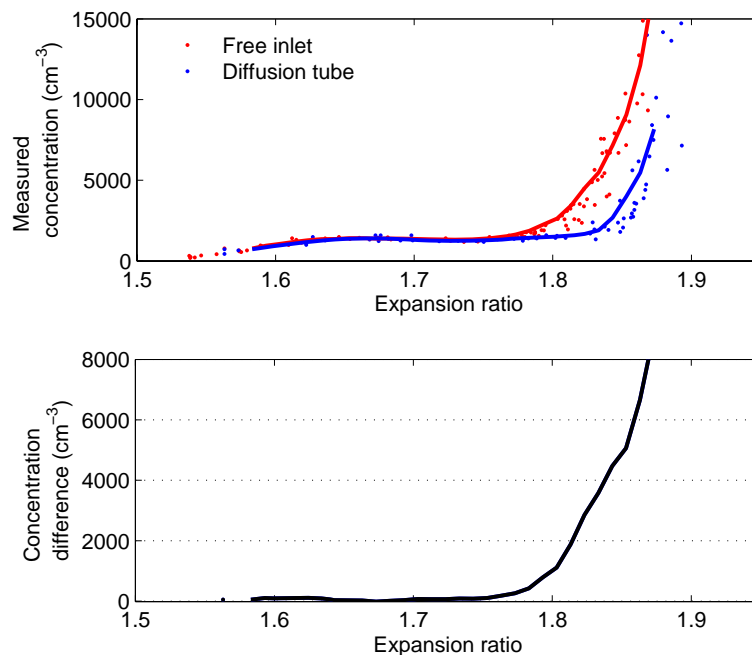


Fig. 8. Expansion scan experiment on 28 May 2007 at 07:50–08:20. Butanol is used as the condensing vapour. The upper panel shows the detected signal with the free inlet (red dots) and with the diffusion tubes (blue dots). Data resulting from subtraction of the two signals is presented in lower panel.

[Title Page](#)[Abstract](#)[Introduction](#)[Conclusions](#)[References](#)[Tables](#)[Figures](#)[◀](#)[▶](#)[◀](#)[▶](#)[Back](#)[Close](#)[Full Screen / Esc](#)[Printer-friendly Version](#)[Interactive Discussion](#)

EGU

Atmospheric cluster
measurements

M. Sipilä et al.

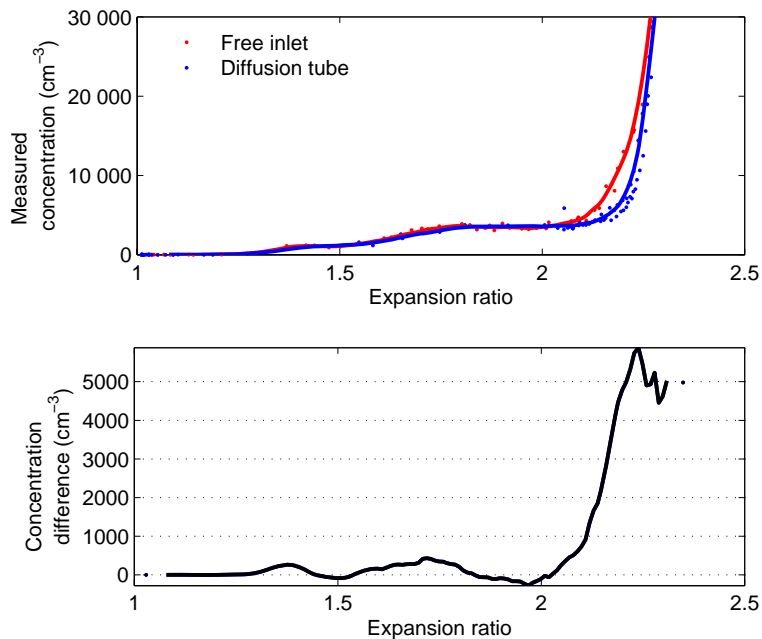


Fig. 9. Data displayed as in Fig. 10 for expansion scan experiment on 28 May 2007 at 11:02–11:33. Water is used as the condensing vapour.

[Title Page](#)[Abstract](#)[Introduction](#)[Conclusions](#)[References](#)[Tables](#)[Figures](#)[◀](#)[▶](#)[◀](#)[▶](#)[Back](#)[Close](#)[Full Screen / Esc](#)[Printer-friendly Version](#)[Interactive Discussion](#)

EGU

**Atmospheric cluster
measurements**

M. Sipilä et al.

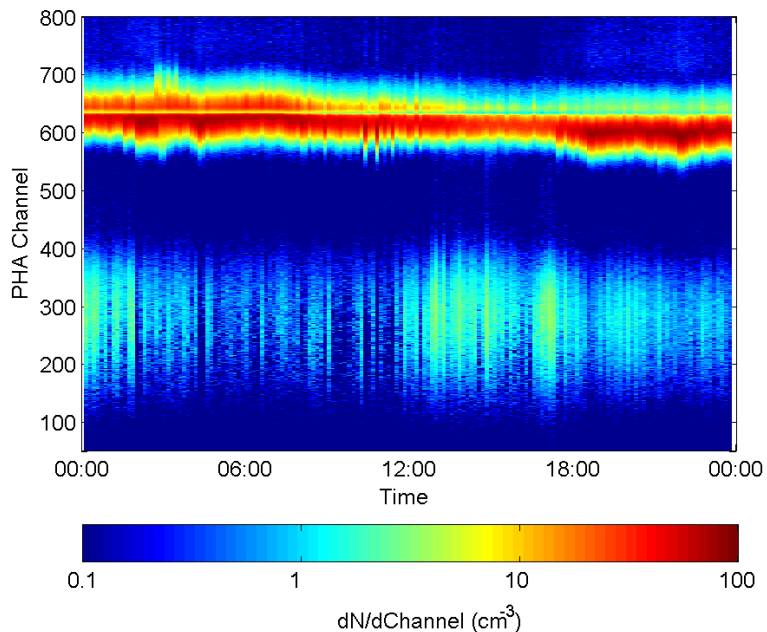


Fig. 10. Pulse height spectra recorded during a non-event day (12 June 2007). Large particles are accumulating in the channels around 600. Clusters are seen around channel 300. Detection efficiency or losses are not taken into account. Gap around channel 650 is an instrumental artefact.

[Title Page](#)[Abstract](#)[Introduction](#)[Conclusions](#)[References](#)[Tables](#)[Figures](#)[◀](#)[▶](#)[◀](#)[▶](#)[Back](#)[Close](#)[Full Screen / Esc](#)[Printer-friendly Version](#)[Interactive Discussion](#)

Atmospheric cluster
measurements

M. Sipilä et al.

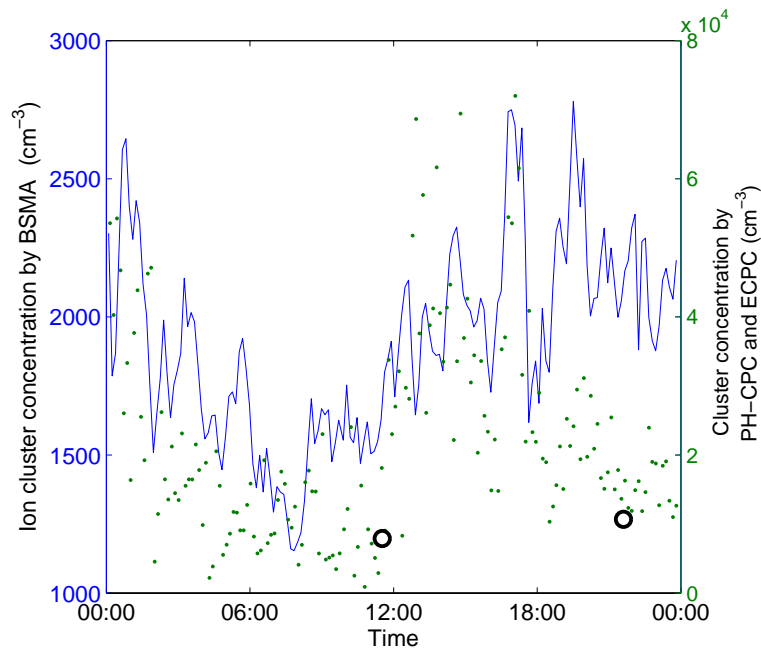


Fig. 11. Total cluster concentration measured by the PH-CPC (green dots) and the E-CPC using butanol as working fluid (black circles), and ion cluster concentration measured by the BSMA (blue line) on 12 June 2007. Detection efficiency of 2% is assumed for the PH-CPC and 12% for the E-CPC. PH-CPC and BSMA signals seem to correlate with each other. Variation in the PH-CPC signal, however, is much larger than in the BSMA.

[Title Page](#)[Abstract](#)[Introduction](#)[Conclusions](#)[References](#)[Tables](#)[Figures](#)[◀](#)[▶](#)[◀](#)[▶](#)[Back](#)[Close](#)[Full Screen / Esc](#)[Printer-friendly Version](#)[Interactive Discussion](#)

EGU